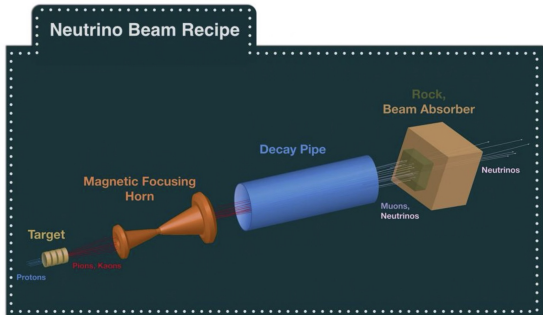
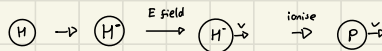


Experimental Setup

Neutrino Beam production



Neutrino beam is made by firing protons at a Beryllium target. Protons are generated by adding an extra electron to hydrogen. This allows it to be accelerated. The electrons are then ripped off, leaving accelerated protons.



The protons are fired at a fixed Beryllium target. Beryllium is chosen due to its low atomic number. A lower atomic number reduces the amount of incoming particles interacting with orbiting electrons. This would produce unwanted secondary particles that would disrupt the neutrino beam manufacturing process.

This interaction produces Pions and kaons.

The magnetic focusing horn focus the pions and kaons into a beam. They then decay into ν_n electrons and muons.

This beam is fired at a thick wall to block all particles apart from the ν_n to get a pure beam.

The resulting neutrino beam is then aimed at the LArTPC.

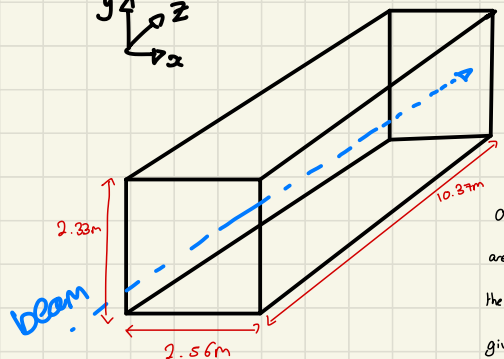
LArTPC

The liquid Argon tank is ~ 470 m from the neutrino production.

Liquid Argon is used for the following reasons:

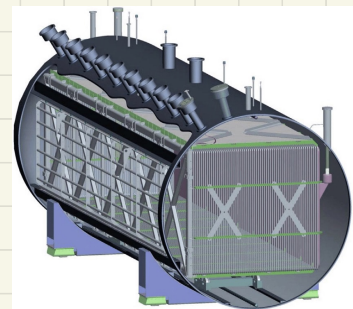
- A noble gas is needed as it is unreactive. This means it won't react with the wire planes or the walls of the tank. This would produce unwanted interactions and background events.
- Argon is relatively dense noble gas $\text{Ne} < \text{Ar} < \text{Kr} < \text{Xe}$
- It is relatively cheap and abundant
- It is easy to purify (impurities are frozen out at its boiling point)
- It is a good insulator which means it is suitable for use alongside the high voltage.
- Has a reasonable boiling point

However, its boiling point at ~ 10 K requires Cryogenics



← Dimensions of the detecting area inside tank

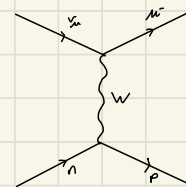
Note that the fiducial volume is 90% of this volume.
Only events within the fiducial volume are used as these are not subject to the edge effects of the system which would give less accurate reconstruction.



As the neutrino beam enters the liquid argon some neutrinos will interact with the argon nuclei: $\bar{\nu}_e + \text{Ar} \rightarrow \text{P} + \bar{\nu}_e$

Neutrinos can undergo many other interactions. Such as: electron-neutrino scattering

However neutrino-electron scattering is not relevant due to a low density of electrons in the tank.



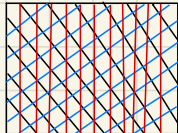
The charged particles emitted from this reaction will ionise the liquid argon producing electrons.

A negative voltage is applied across the tank. So the electrons will drift towards one side of the tank.

Scintillation photons are also emitted as the charged particles propagate. These act as a trigger for signal events.

The electrons are collected by the wire planes.

3 wire planes are used in the following geometry:



The same result could be achieved using 2 wires, however the use of 3 means the detector still works if any wire breaks. Also it enables the system to be more precise without moving the wires closer together as this would cause interference between the wires in the same plane.

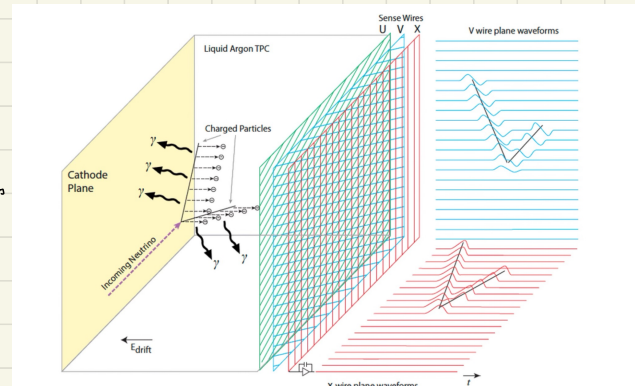
The properties of the neutrino are then reconstructed using the angle between the products of the reaction and the length of the path.

However, the signal tracks are not the only signal.

Examples of background events are:

- Electron neutrino events from solar neutrinos
- Cosmic muons
- Neutral current events.

Therefore, the data needs to be cleaned.



2 Flavour oscillation Probability

↓
flavor
 $|\nu(t=0)\rangle = |\nu_\alpha\rangle = \cos\theta|\nu_1\rangle + \sin\theta|\nu_2\rangle$

↓
mass
 $|\nu(t)\rangle = e^{i\frac{E}{2E}t} \cos\theta|\nu_1\rangle + e^{i\frac{E}{2E}t} \sin\theta|\nu_2\rangle$

Doys (1-2)

$$P(|\nu_\alpha \rightarrow \nu_\beta\rangle) = |\langle \nu_\beta | \nu(t) \rangle|^2 = \left| (-\sin\theta \langle \nu_1 | + \cos\theta \langle \nu_2 |) (e^{i\frac{E}{2E}t} \cos\theta |\nu_1\rangle + e^{i\frac{E}{2E}t} \sin\theta |\nu_2\rangle) \right|^2$$

$$\begin{aligned}
 &= \left| -\sin\theta \cos\theta e^{i\frac{E}{2E}t} \langle \nu_1 | \nu_1 \rangle - e^{i\frac{E}{2E}t} \sin^2\theta \langle \nu_1 | \nu_2 \rangle + e^{i\frac{E}{2E}t} \cos^2\theta \langle \nu_2 | \nu_1 \rangle + \cos\theta \sin\theta e^{i\frac{E}{2E}t} \langle \nu_2 | \nu_2 \rangle \right|^2 \\
 &= \left| -\frac{1}{2} \sin 2\theta e^{i\frac{E}{2E}t} + \frac{1}{2} \sin 2\theta e^{i\frac{E}{2E}t} \right|^2 \quad \text{Orthogonal} \\
 &= \left| \frac{1}{2} \sin 2\theta (e^{i\frac{E}{2E}t} - e^{i\frac{E}{2E}t}) \right|^2 \\
 &= \left| \frac{1}{2} \sin 2\theta \left(e^{i\frac{m_2^2 L}{2E}} - e^{i\frac{m_1^2 L}{2E}} \right) \right|^2 \\
 &= \frac{1}{4} \sin^2 2\theta \left| e^{i\frac{m_2^2 L}{4E}} \left(e^{i\frac{m_2^2 L}{4E}} - e^{i\frac{m_1^2 L}{4E}} \right) \right|^2 \\
 &= \frac{1}{4} \sin^2 2\theta \left| e^{i\frac{m_2^2 L}{4E}} \frac{1 - e^{i\frac{m_2^2 L}{4E}}}{1 - e^{i\frac{m_1^2 L}{4E}}} \left(\frac{i(m_2^2 - m_1^2)L}{4E} - \frac{i(m_2^2 - m_1^2)L}{4E} \right) \right|^2 \\
 &= \frac{1}{4} \sin^2 2\theta \left| \frac{2i \sin\left(\frac{\Delta m^2 L}{4E}\right)}{1 - e^{i\frac{m_1^2 L}{4E}}} \right|^2
 \end{aligned}$$

$$P^2 = E_i^2 - \eta_i^2$$

$$P = E_i \left(1 - \frac{\eta_i^2}{E_i^2}\right)^{\frac{1}{2}}$$

$$\approx E_i \left(1 - \frac{\eta_i^2}{E_i^2}\right)$$

$$P \approx E - \frac{\eta_i^2}{2E_i}$$

$$q_{i,\infty} = E_i t - P_i \infty \quad P_i \infty$$

$$q_{i,\infty} = E_i t - E_i \infty + \frac{P_i^2}{2E_i} \infty$$

Assume $t \gg \infty$

$$q_{i,\infty} = \frac{m_i^2}{2E_i} \infty$$

L: length to detector (km)

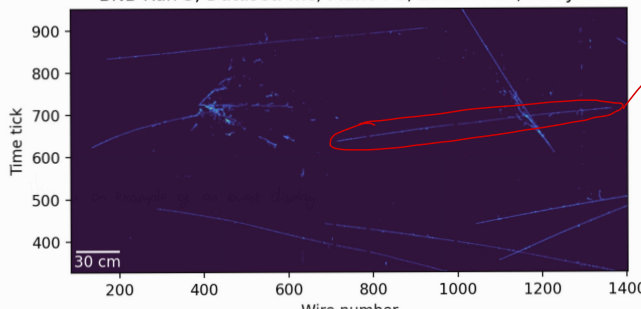
E: Energy of neutrino (GeV)

Δm^2 : mass difference between neutrinos (eV)

θ : mixing angle between the flavor eigenstates

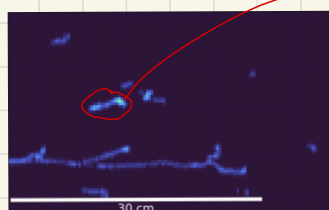
Event Displays

BNB Run 3, Dataset: mc, Plane : V, Event: 267, Entry: 2



For example this is probably a cosmic muon.
The track is long which suggests it is high energy.
and the particle is massive as it isn't scattered

Zooming in on some smaller events:



This is perhaps a signal event as it is short and has 2 branches.
However, could also be an ve event.

This is an example of an event display, this includes the signal events as well as background.

Some paths can be categorised by eye however this is a long and inaccurate process.

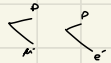
It is also easy to distinguish an electron neutrino event from a muon neutrino event.

This is because electron neutrinos will produce an electron which can shower (it has high energy).

So comparing high energy ν_e and ν_μ events:



However, at low energies, the electrons don't have enough energy to shower so the paths look similar:



Events

Category	Interaction
4	Cosmic
5	Out Fid. Vol.
7	EXT
10	ν_e CC
21	ν_μ CC
31	ν NC

Table 3: Different categories with respect to their interactions

• NC interactions are background as ν_e and ν_μ events can't be distinguished. Also the NC has a smaller σ so the disregarded events are a big fraction

↳ for the energy $g \sim \text{GeV}$ $\sigma_{\text{NC}} \sim 10 \sigma_{\text{CC}}$

• ν_e CC are background as the beam is ν_μ so the ν_e events don't come from the beam.

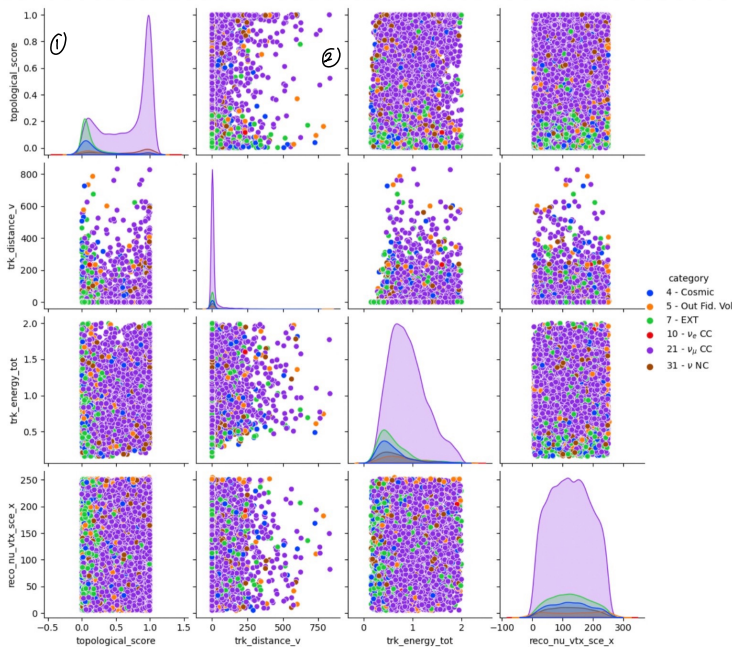
• Outside Fiducial volume may be influenced by edge effects. So are rejected for accuracy.

• EXT are events measured by the detector

• Cosmic are Cosmic events introduced by MC.

Note that electrons show as they are low mass which means they lose energy to the medium much more (it interacts more with the medium)

Event Properties

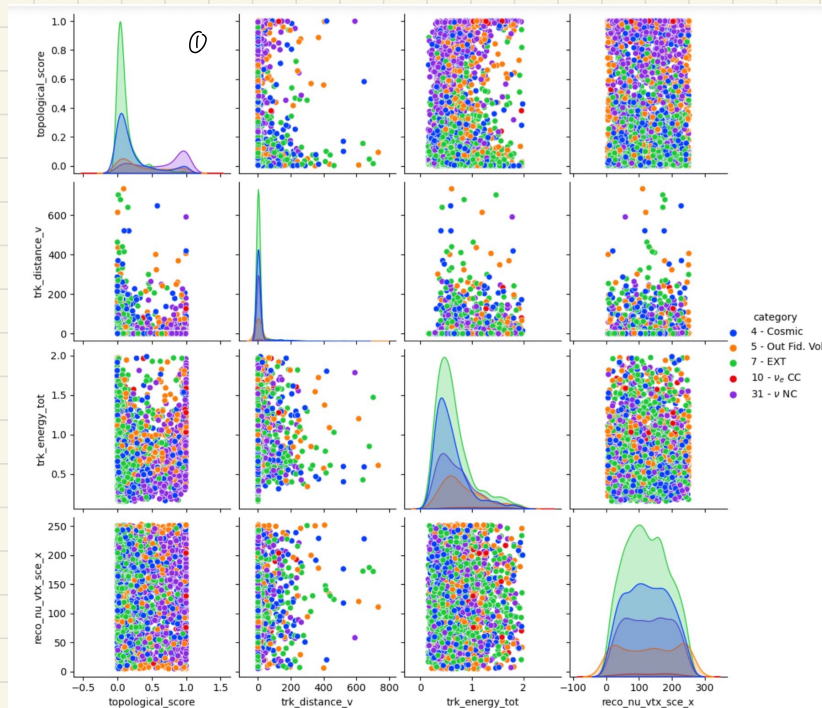


① => Topological score digits how certain each event fits into its category
 Category => Majority of v_μ CC events we see $\sim 95\%$
 Certain they are v_μ CC \rightarrow high energy
 However, still a large number of events with a low topological score \rightarrow not certain it is v_μ CC \rightarrow low energy

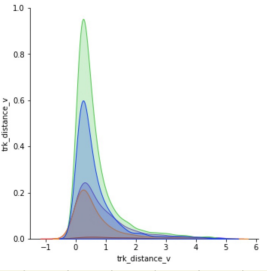
Also very low topological score for EXT \rightarrow this is because had to tell this apart from Cosmic

- ② • High probability that v_μ CC travels a short distance (high density \Rightarrow pure top log) \Rightarrow makes sense
 • Orange/blue with low TS (bad track) \Rightarrow green (purple) blue
 • low density of purple far right \Rightarrow mostly only v_μ CC travel far

Removing the v_μ CC data to get a clear look at the background (looking at trend)



- ① • Cosmic + EXT hard to disentangle (low TS)
 • v NC distinctive (recording nucleus shown)
 • Can also be confused with v CC which explains 2 local maxima
 • OFV \rightarrow vertex outside FV so low TS



Enlarging the distance Histogram
 mean the data can be seen better, we can see that almost all of the remaining clusters travel < 1 cm

Come back to Exercise 5

We removed the ν_e CC and ν_μ CC processes from the Monte Carlo data.

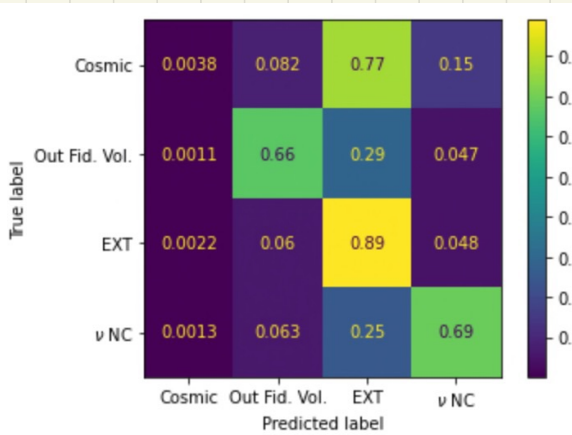
Days (3-4)

This was then split 80:20 into training data and testing data.

We started with a 10% of the data, 1000 trees and max depth 8.

This gave a training accuracy $\sim 70\%$ } these are fairly constant \rightarrow no overfitting
and a test accuracy $\sim 65\%$ }

To gauge how good the model is, we look at the Confusion matrix:



This shows how well the model predicts the classification of the data.

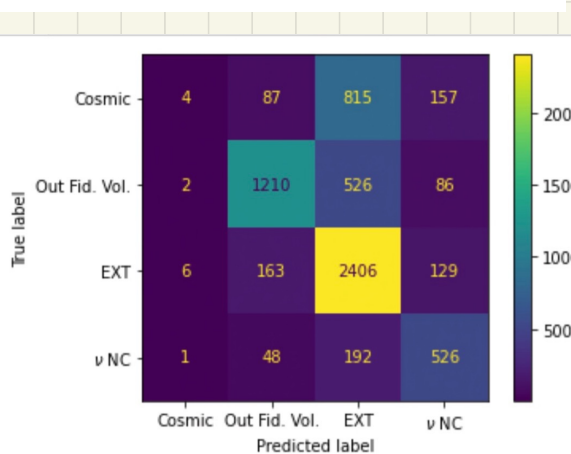
For example, it correctly classifies 89% of the EXT data.

To this corresponds to 2406 events.

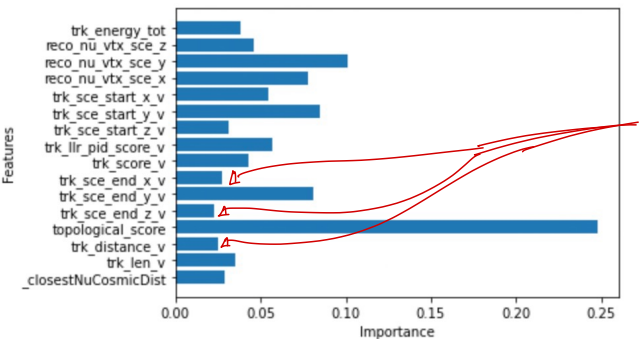
↳ Both very similar events (big, high energy)

It can also be seen that the model hardly ever classifies as Cosmic despite ~ 1000 Cosmic events.

The model is reasonable for ν NC, 25% of the time it falsely identifies it as EXT \rightarrow high energy Cosmic



Falsely identifies ν FV as EXT 30%



The most important factor is topological score.
 Could potentially remove the least important factors to try improve accuracy = could be confusing the model.

This machine learning process is not right yet but is used later.

Cutting data

Looking at the monte Carlo data, we need to try and reduce the number of background events.

This is done by making Selection Cuts. These Cuts can then also be made to the real data.

The aim is to make a pure dataset of ν_{μ} . The purer the dataset, the better the oscillation probability equation will apply.

However, a large amount of data is still required as it is a statistical process \rightarrow more data, the less randomness.

A highlight of cuts made:

- Disregarded any particle with $E > 2$ GeV \rightarrow these are unphysical. \rightarrow neutrino beam doesn't produce neutrinos this energetic.
- Cut out start points <-100 or >100 in the y direction \rightarrow Colm's muons are strongest from vertical direction
 \rightarrow these will have start points close to edges of detector.
- Same logic applies to the end point.
- Disregarded $E < 0.4$ GeV \rightarrow Majority of this was background. Why?
- Disregarded topological score < 0.2 \rightarrow this is the region with most Earth and cosmic \rightarrow these get confused
- Disregarded $\text{reco} > 240$ or <10 . These are ODF \rightarrow not from beam
- Disregarded track score < 0.7 . \rightarrow not likely to actually be a track \rightarrow rubbish data.

After making all of the selection cuts (with some altering)

We managed to achieve a purity of 89.64% as opposed to the original purity of the dataset of 42.15%

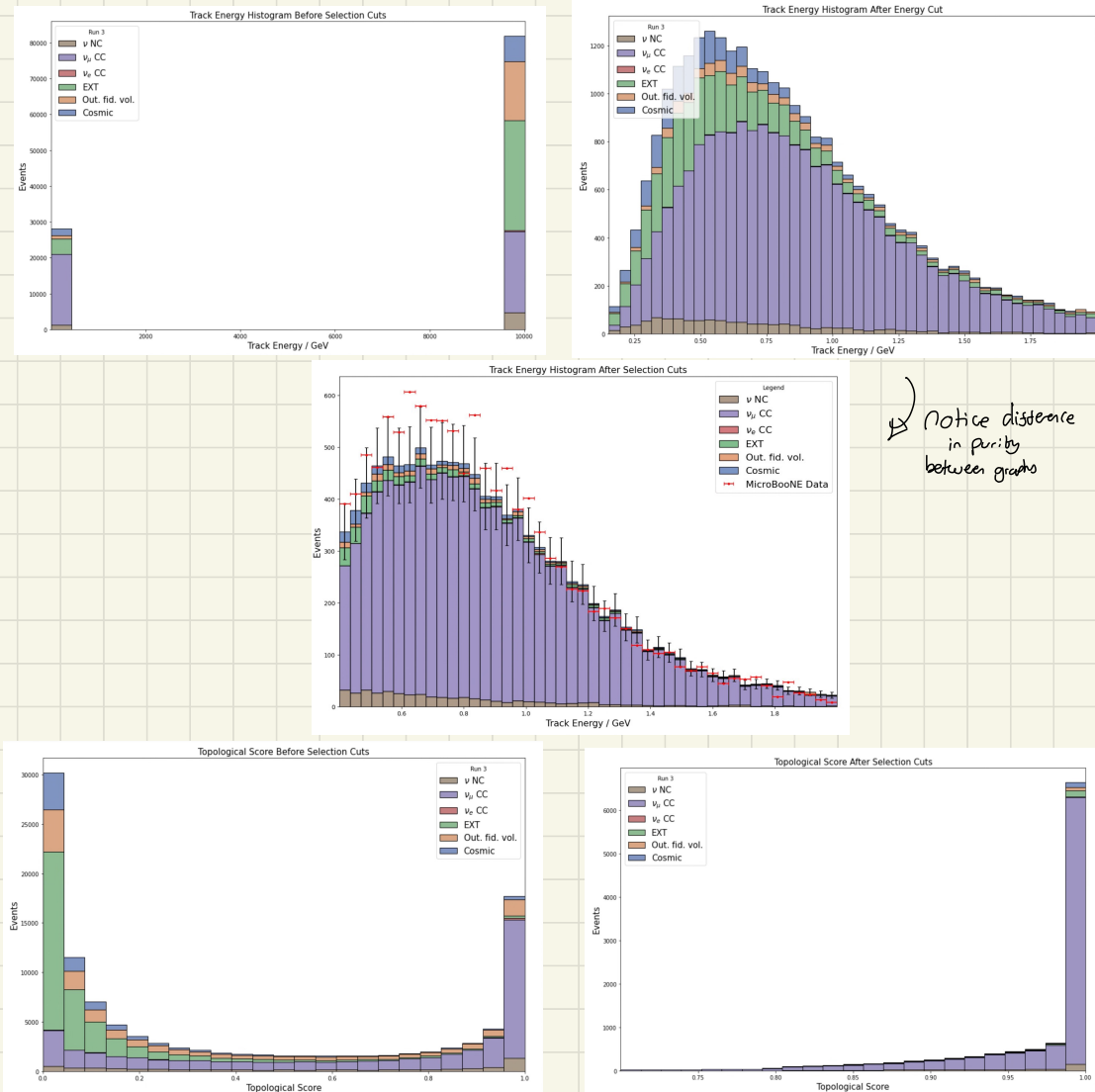
However, this high purity came at a sacrifice of an efficiency of 10.77%.

But this efficiency was not true to the experiment due to a large number of events with unphysically high energies as shown below.

As this was relevant data, we took this out and disregarded it from subsequent calculations.

Using this new initial dataset, the efficiency of the selection cuts was 45.53%.

Also, this means that the original purity of the dataset was 72.87%.



Notice difference
in purity
between graphs

For example, the Topological Score graphs above demonstrate why we initially chose to delete data with a topological score < 0.2 as this was primarily background events.

With regards to the energy graph, we made the same selection cuts to the real microBoone data (red data points).

The Monte Carlo data has 2 errors:

- A 15% Systematic error

- A \sqrt{N} Poisson error where N is the number of counts.

These errors were propagated in quadrature: $\sigma_{\text{sys}} = \sqrt{(\sigma_{\text{stat}})^2 + (\sigma_{\text{sys}})^2}$

For large counts (eg around peak, ~ 600 counts) the systematic error dominated.

At low counts the Poisson error becomes relevant.

So for this part of the experiment the systematic error was dominant.

The origin of this Systematic error is:

- Underlying error in physical constants eg cross sections
- The simulation will be simplified compared to the complex system.

This cannot be reduced in our control.

However, for the bins with low counts the statistical error is relevant.

More data will reduce this error.

Oscillation fitting

Day 2 (S-6)

Before we derived the probability of a ν_{μ} oscillating to a ν_e in a 2 flavour system:

$$P(\nu_{\mu} \rightarrow \nu_e) = \sin^2(2\theta) \sin^2\left(1.27 \frac{\Delta m^2_{31} (\text{eV}^2) L (\text{km})}{E (\text{GeV})}\right)$$

So the probability of a ν_{μ} not oscillating to a ν_e is: $P(\nu_{\mu} \rightarrow \nu_{\mu}) = 1 - \sin^2(2\theta) \sin^2\left(1.27 \frac{\Delta m^2_{31} (\text{eV}^2) L (\text{km})}{E (\text{GeV})}\right)$

The length is a known quantity: $L = 0.47 \text{ km}$

The energy is the energy of each bin \Rightarrow known

Δm^2_{31} and θ_{23} are the unknown quantities that we are fitting for.

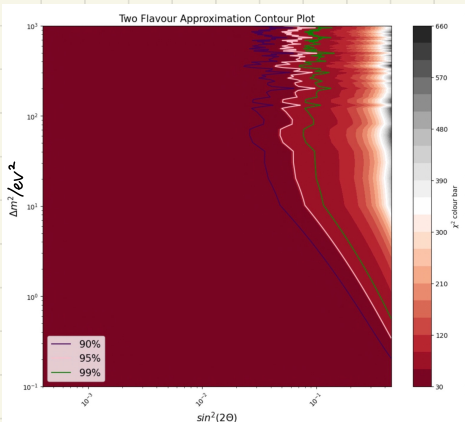
We applied the probability to not oscillate to the energy plot for a range of θ_{23} and Δm^2_{31} .

The χ^2 was calculated at each parameter pair using:

$$\chi^2 = \sum_{i=1}^n \left(\frac{(\mu_i - M_i)^2}{\sigma_i^2} \right)$$

where μ_i is the MC counts
 M_i is the data counts
 σ_i is the error, } in each bin i .

A χ^2 Contour plot was plotted for the parameter space:



Note the sinusoidal behaviour of the contours in Δm^2 .

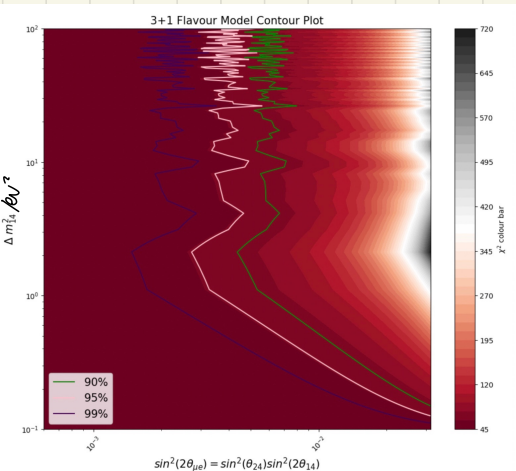
This makes sense as it is inside the sin.

Also note how it changes due to the log scale.

Therefore, the values along each Confidence level are the 'accepted' values.

Using the relation explained and derived above, the Confidence region can be propagated into the 3+1 flavour model

the χ^2 Contour plot for this is shown below.



The Confidence levels that we have derived can be directly compared to the possible values of Δm^2_{41} and $\sin^2(2\theta_{41})$ found by LSND and MiniBoone.

If our Confidence levels are to the left of the possible parameter then we can reject the value and the 3+1 model.

A plot of this is shown below

The 90%, 95% and 99% Confidence levels are shown.

These are the values of χ^2 that define what values of Δm^2_{41} and $\sin^2(2\theta_{41})$ can be rejected.

For example, all parameter values to the right of the 99% Confidence level can be rejected with 99% certainty.

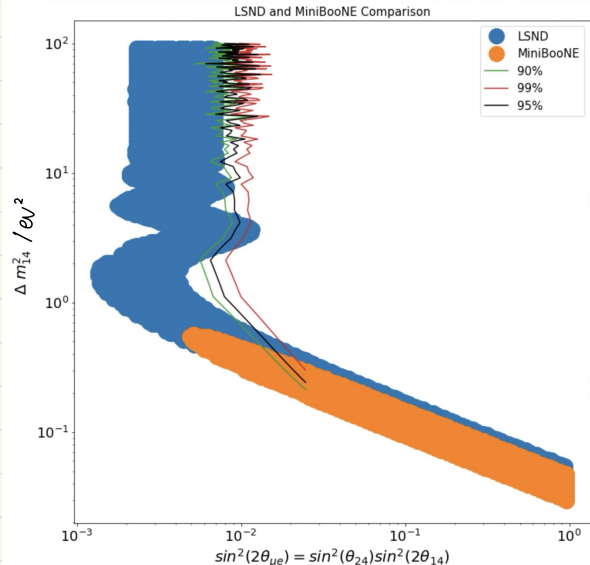
However, all values to the left the experiment is not sensitive to. This is due to the large contours. This is due to the log scale.

This Confidence level can be shifted to the left by

$$\text{Using: } \sin^2(2\theta_{41}) : \frac{\sin^2(2\theta_{41})}{1 + \sqrt{1 - \sin^2(2\theta_{41})}} \left[1 \pm \sqrt{1 - \sin^2(2\theta_{41})} \right]$$

This is propagating our known Confidence regions into the 3+1 flavour domain to reject proposed values

from LSND and MiniBoone for Δm^2_{41} and $\sin^2(2\theta_{41})$



At this current point we reject very few values that LSND and miniboone accepted.

Therefore, we need to modify our experiment to reject more values.

Our first method for this was to increase the number of bins in our histogram.

This will increase the degrees of freedom which will make the experiment sensitive to more parameter values. \Rightarrow Note that $\text{DoF} = N - 2$ (2 free parameters)

However, we do not want to overbin the data as the histogram will have too few counts per bin and will be subject to random fluctuations.

To quantify this we used the M statistic.

This is defined as:

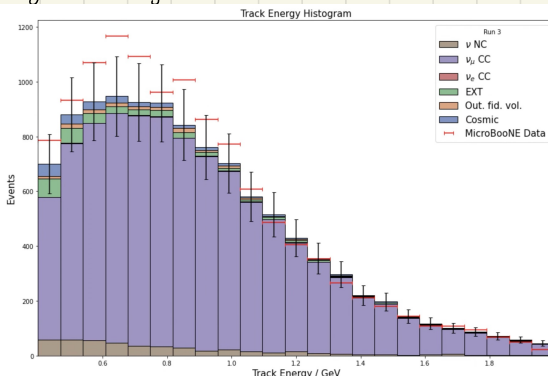
$$M_x = \frac{\log N}{H_x} \quad \text{where } H_x = \log\left(\frac{N}{N_{\text{true}}}\right) + 1$$

If $M_x < 2$ then the histogram is underbinned \rightarrow will be subject to random fluctuations

If $M_x > 3$ then the histogram is overbinned \rightarrow miss out on important features (oversmooth)

$M = 2$ is the best value we can use

Before we were using 23 bins, this is shown below:



Note that the M value for 23 bins was 2.27

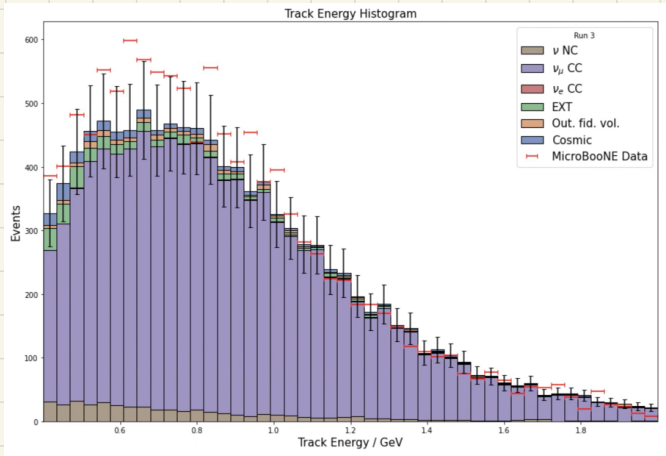
Therefore this was neither underbinned or overbinned.

However, there is room to increase the number of bins before it is overbinned.

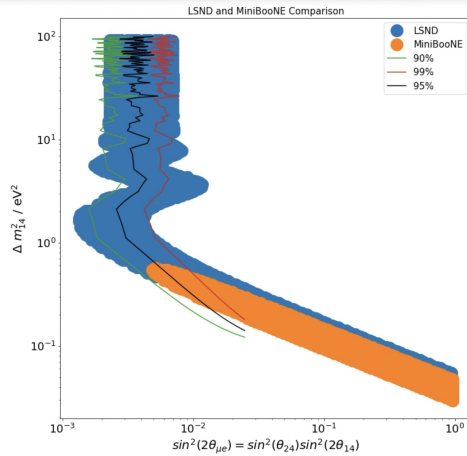
With 46 bins the M value was 2.0001

Therefore this was the highest number of bins we could use before the data was overbinned.

This is shown below.



This gave the following effect to the confidence levels:



These new Confidence levels reject many more values than before.

We can fully reject all of MiniBooNE's parameters with 90% confidence. And we can reject almost all of the LSND values with 90% confidence.

However, we aim to reject more values at a higher confidence level.

3+1 Oscillation derivation for above conversion

$$P(\alpha \rightarrow \beta) = \delta_{\alpha\beta} - 4(\delta_{\alpha\beta} - U_{\alpha 4}^* U_{\alpha 4}) U_{\beta 4} U_{\beta 4}^* \sin^2 \left(1.27 \frac{\Delta m_{14}^2 L}{E} \frac{(\text{eV}^2)(\text{km})}{(\text{GeV})} \right) \quad (12)$$

$$= \delta_{\alpha\beta} - \sin^2(2\theta_{\alpha\beta}) \sin^2 \left(1.27 \frac{\Delta m_{14}^2 L}{E} \right).$$

$$P(\mu \rightarrow \mu) = S_{\mu\mu} - 4 \left(S_{\mu\mu} - U_{\mu 4}^* U_{\mu 4} \right) U_{\mu 4} U_{\mu 4}^* \sin^2 \left(1.27 \frac{\Delta m_{14}^2 L}{E} \right)$$

$$= 1 - 4 \left(1 - |U_{\mu 4}|^2 \right) |U_{\mu 4}|^2 \sin^2 \left(1.27 \frac{\Delta m_{14}^2 L}{E} \right)$$

$$1 - \sin^2(2\theta_{\mu\mu}) \sin^2 \left(1.27 \frac{\Delta m_{14}^2 L}{E} \right)$$

$$4 \left(1 - |U_{\mu 4}|^2 \right) |U_{\mu 4}|^2 = \sin^2(2\theta_{\mu\mu})$$

$$|U_{e4}|^2 = \sin^2 \theta_{14},$$

$$|U_{\mu 4}|^2 = \sin^2 \theta_{24} \cos^2 \theta_{14}.$$

$$\underline{4 \left(1 - \sin^2(\theta_{24}) \cos^2(\theta_{14}) \right) \sin^2(\theta_{24}) \cos^2(\theta_{14})} = \sin^2(2\theta_{\mu\mu})$$

$$P(e \rightarrow e) = 1 - 4 \left(1 - |U_{e4}|^2 \right) |U_{e4}|^2 \sin^2 \left(1.27 \frac{\Delta m_{14}^2 L}{E} \right)$$

$$= 1 - \sin^2(2\theta_{ee}) \sin^2 \left(1.27 \frac{\Delta m_{14}^2 L}{E} \right)$$

$$4 \left(1 - \sin^2(\theta_{14}) \right) \sin^2(\theta_{14}) = \sin^2(2\theta_{ee})$$

$$4 \left(\cos^2(\theta_{14}) \sin^2(\theta_{14}) \right) = \sin^2(2\theta_{ee})$$

$$4 \left(\frac{1}{2} \sin(2\theta_{14}) \right)^2$$

$$\underline{\sin^2(2\theta_{14}) = \sin^2(2\theta_{ee}) = 0.24}$$

$$P(\mu \rightarrow e) = -4 |U_{\mu e}|^2 |U_{e4}|^2 = -\sin^2(2\theta_{\mu e})$$

$$\sin^2(2\theta_{\mu e}) = 4 \sin^2(\theta_{24}) \cos^2(\theta_{14}) \sin^2(\theta_{14})$$

$$= 4 \sin^2(\theta_{24}) \left(\frac{1}{2} \sin^2(2\theta_{14}) \right)^2$$

$$\underline{\sin^2(2\theta_{\mu e}) = \sin^2(\theta_{24}) \sin^2(2\theta_{14})}$$

Need to remove $\sin^2(\theta_{24})$ for $\sin^2(2\theta_{14})$ and $\sin^2(2\theta_{34})$

$$4(1 - \sin^2(\theta_{24}) \cos^2(\theta_{14})) \sin^2(\theta_{24}) \cos^2(\theta_{14}) = \sin^2(2\theta_{14})$$

$$4 \sin^2(\theta_{24}) \cos^2(\theta_{14}) - 4 \sin^4(\theta_{24}) \cos^4(\theta_{14}) - \sin^2(2\theta_{14}) = 0$$

$$\sin^4(\theta_{24}) - \frac{\sin^2(\theta_{24})}{\cos^2(\theta_{14})} + \frac{\sin^2(2\theta_{14})}{4 \cos^4(\theta_{14})} = 0 \quad \checkmark \quad (\div 4 \cos^4(\theta_{14}))$$

$$x^2 - \frac{1}{\cos^2(\theta_{14})} x + \frac{\sin^2(2\theta_{14})}{4 \cos^4(\theta_{14})} = 0 \quad \checkmark$$

$$\sin^2(\theta_{24}) = \frac{1}{\cos^2(\theta_{14})} \pm \sqrt{\frac{1}{\cos^4(\theta_{14})} - \frac{\sin^2(2\theta_{14})}{\cos^2(\theta_{14})}}$$

$$= \frac{1}{2 \cos^2(\theta_{14})} \pm \frac{1}{2 \cos^2(\theta_{14})} \sqrt{1 - \sin^2(2\theta_{14})}$$

$$= \frac{1}{2 \cos^2(\theta_{14})} \left[1 \pm \sqrt{1 - \sin^2(2\theta_{14})} \right] \checkmark$$

$$\cos(2\theta_{14}) = 2\cos^2(\theta_{14}) - 1$$

$$2\cos^2(\theta_{14}) = \cos(2\theta_{14}) + 1$$

$$= \sqrt{1 - \sin^2(2\theta_{14})} + 1$$

$$2\cos^2(\theta_{14}) = \cos(2\theta_{14}) + 1$$

$$= \sqrt{1 - \sin^2(2\theta_{14})} + 1$$

$$= \frac{1}{\sqrt{1 - \sin^2(2\theta_{14})} + 1} \left[1 \pm \sqrt{1 - \sin^2(2\theta_{14})} \right]$$

$$\sin^2(\theta_{24}) = \frac{1}{1 + \sqrt{1 - \sin^2(2\theta_{14})}} \left[1 \pm \sqrt{1 - \sin^2(2\theta_{14})} \right]$$

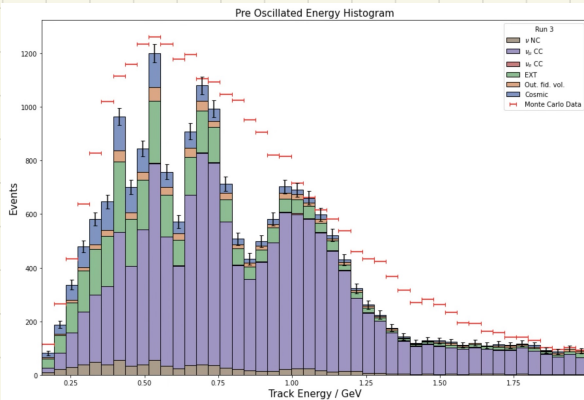
$$\sin^2(2\theta_{14}) = \frac{\sin^2(2\theta_{14})}{1 + \sqrt{1 - \sin^2(2\theta_{14})}} \left[1 \pm \sqrt{1 - \sin^2(2\theta_{14})} \right]$$

Checking

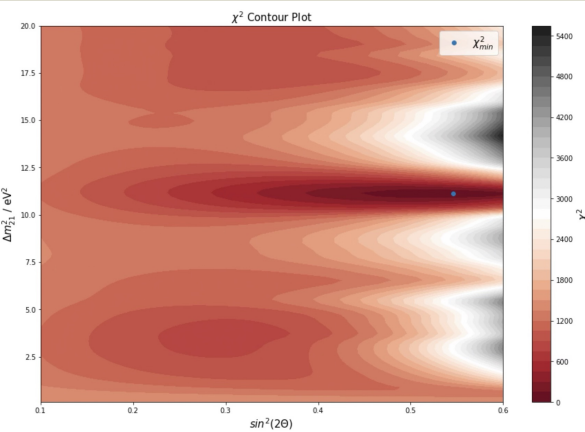
Days (7-8)

To check that our analysis was valid we took data that had already been propagated with definite values of Δm^2_{31} and $\sin^2(2\theta)$ and performed a χ^2 minimization to find the parameters that we applied.

The data after the oscillation process is shown below:



The χ^2 Contour plot for a range of Δm^2_{31} and $\sin^2(2\theta)$:



To find errors on our parameters we plotted the Contours for $\chi^2_{\min} + 1$:

Note that no selection cuts have been made apart from $E < 2$ GeV

This is because all data was propagated the other way and the more data the better

Also note that the systematic error is removed here

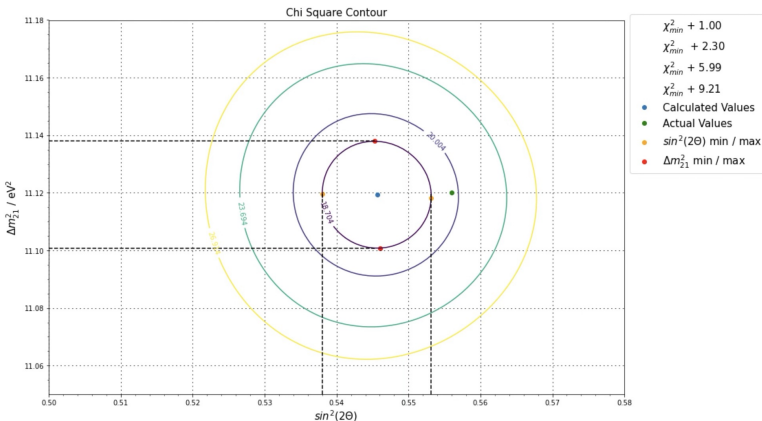
Now we have found a value of Δm^2_{31} and $\sin^2(2\theta)$ which minimizes the χ^2 .

The values we found were:

$$\Delta m^2_{31} = 11.119 \text{ eV}^2$$
$$\sin^2(2\theta) = 0.546$$

with a $\chi^2 = 17.704$

which gave $\chi^2_{\text{red}} = 0.402$.



The values of $\sin^2(2\theta)$ and Δm_{21}^2 at $\chi^2_{\min} + 1$ correspond to $\Delta m_{21}^2 \pm \sigma_{\Delta m_{21}^2}$.

(68%)?

Therefore the difference between Δm_{21}^2 min and max divided by 2 corresponds to the error.

The same applies to $\sin^2(2\theta)$.

This gives:

- $\sin^2(2\theta) = 0.546 \pm 0.008$
- $\Delta m_{21}^2 = 11.119 \pm 0.019$

The actual values that produced the oscillations are:

- $\sin^2(2\theta) = 0.556$
- $\Delta m_{21}^2 = 11.120$

Therefore, our value for $\sin^2(2\theta)$ strongly agrees but Δm_{21}^2 differs.

However it does agree within 1σ so we accept that our model works.

Applying Machine Learning

Using our previous selection cuts we achieved an efficiency of 45.53% and a purity of 89.64%.

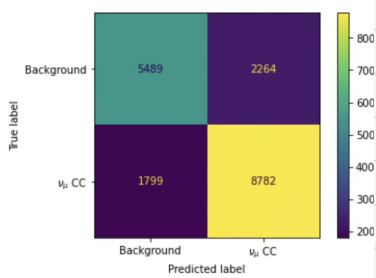
We used machine learning to try to get a higher efficiency (thus more data) whilst maintaining a high purity.

To achieve this we:

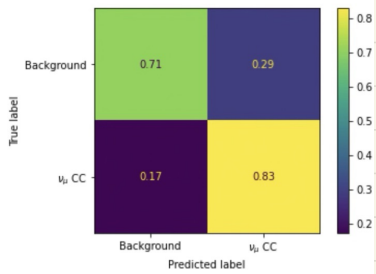
- Categorised all backgrounds into one event
- made the sample size of signal and background events ~~regular~~

This gave an accuracy on the training set of 78.55%
As these are close we are not
testing set of 77.84% overfitting

To display how accurate the model is on Background and Signal we use confusion matrices:

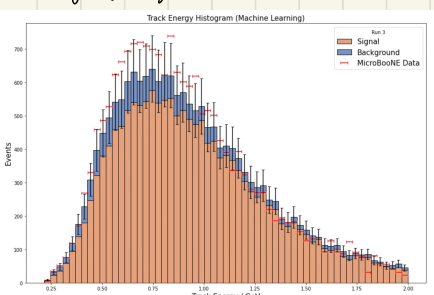


This shows that it correctly identifies 71% of backgrounds and 83% of signal events.



Advancing with this model we then apply it to the whole data set.

The Histogram for tracks is shown below.



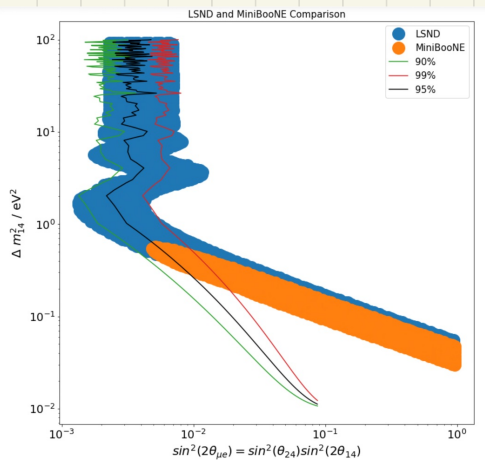
Quantitatively, this new data has a purity of 88.69% (very similar to before)

However, it has an efficiency of 68.33% (much better than before)

This means we have much more data at the same points.

Therefore, we can plot our histogram with more bins which should reject more LSND proposed parameter values.

So plotting the new χ^2 Contours:



Although it is hard to see, the contours have slightly moved

This is expected and a positive result.

At 90% Confidence Almost all parameters are rejected

3 flavour oscillation

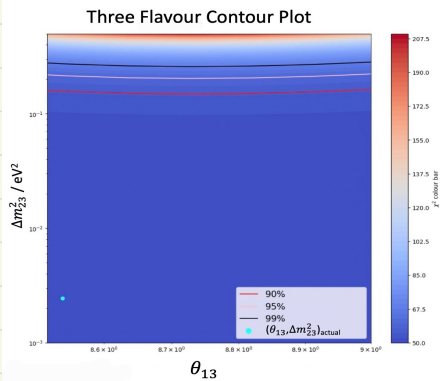
Beyond LSND

We also investigated the 3 flavour model to solidify our results.

The value of θ_{13} is known very precisely.

Although we cannot produce an exact value of θ_{13} with this data, we can confirm that our model doesn't reject this value. This confirms that our model and analysis doesn't rule out known values which solidifies our method.

So applying the 3 flavour oscillation probability to the mc data as before yields a χ^2 Contour:



All values above the confidence levels can be rejected with the associated confidence.

As can be seen from the graph the actual value of θ_{13} is well within the 'not rejected value'.

However, this doesn't 'accept' the value but this was beyond the limitations of the model.

3 flavour oscillation derivation

$$\begin{aligned}
 P(\nu_\alpha \rightarrow \nu_\beta) &= -4 \sum_{i>j} (U_{\alpha i} U_{\beta i} U_{\alpha j} U_{\beta j}) \sin^2(1.27 \Delta m_{ij}^2 \frac{L}{E}) \\
 &= -4[(U_{\alpha 1} U_{\beta 1} U_{\alpha 2} U_{\beta 2}) \sin^2(1.27 \Delta m_{12}^2 \frac{L}{E}) \cancel{\rightarrow 0} \\
 &\quad + (U_{\alpha 1} U_{\beta 1} U_{\alpha 3} U_{\beta 3}) \sin^2(1.27 \Delta m_{13}^2 \frac{L}{E}) \quad \} \\
 &\quad + (U_{\alpha 2} U_{\beta 2} U_{\alpha 3} U_{\beta 3}) \sin^2(1.27 \Delta m_{23}^2 \frac{L}{E}) \quad \} \text{ equal}
 \end{aligned}$$

$$P(\mu \rightarrow \mu) = 1 - P(\mu \rightarrow e) - P(\mu \rightarrow \tau)$$

$$\begin{aligned}
 P(\alpha \rightarrow \beta) &\stackrel{||}{\approx} [U_{\alpha 1} U_{\beta 1} U_{\alpha 2} U_{\beta 2} + U_{\alpha 2} U_{\beta 2} U_{\alpha 3} U_{\beta 3}] \sin^2(1.27 \Delta m_{23}^2 \frac{L}{E})
 \end{aligned}$$

$$\begin{aligned}
 P(\mu \rightarrow e) &= -4[U_{\mu 1} U_e U_{\mu 2} U_{e 3} + U_{\mu 2} U_{e 2} U_{\mu 3} U_{e 3}] [\dots] \\
 &= -4[(S_{12} C_{23} - C_{12} S_{23}) (C_{13} C_{33}) + (C_{12} C_{33} - S_{12} S_{33}) (S_{13} C_{33})] [C_{13} S_{23} S_{33}] \\
 &= -4[-S_{12} C_{12} C_{13} C_{23} - S_{23} S_{13} C_{12}^2 C_{13} + C_{12} C_{13} C_{23} S_{12} - S_{12}^2 S_{13} S_{23} C_{13}] [C_{13} S_{23} S_{33}] \\
 &= -4[-S_{12} C_{12} C_{23} + C_{12} C_{23} S_{12} - (S_{23} S_{13} C_{12}^2 + S_{23} S_{13} S_{12}^2)] [C_{13}^2 S_{23} S_{13}] \\
 &= -4[-S_{12} C_{12} C_{23} + C_{12} C_{23} S_{13} - S_{23} S_{13}] [C_{13}^2 S_{23} S_{13}]
 \end{aligned}$$

$$\begin{aligned}
 P(\mu \rightarrow e) &= 4 S_{23}^2 C_{13}^2 S_{13}^2 \sin^2(1.27 \Delta m_{23}^2 \frac{L}{E}) \\
 &= 4 \sin^2(\theta_{23}) \cos^2(\theta_{13}) \sin^2(\theta_{13}) \sin^2(\dots)
 \end{aligned}$$

:

$$\begin{aligned}
 P(\mu \rightarrow \tau) &= -4[U_{\mu 1} U_\tau U_{\mu 2} U_{\tau 3} + U_{\mu 2} U_{\tau 2} U_{\mu 3} U_{\tau 3}] \\
 &= -4[(-S_{12} C_{23} - C_{12} S_{23}) (S_{12} S_{13} \cancel{+ C_{12} S_{13} C_{23}}) + (C_{12} C_{23} - S_{12} S_{23}) (-C_{12} S_{13} - S_{12} S_{13} C_{23})] [C_{13}^2 S_{23} C_{23}] \\
 &= -4[\cancel{-S_{12}^2 S_{23} C_{23}} + S_{12} C_{13} C_{23}^2 \cancel{- S_{12}^2 S_{13} + C_{12}^2 S_{13}^2 C_{23}} - C_{12}^2 S_{13}^2 S_{13} + C_{12}^2 S_{13}^2 C_{23} - C_{12}^2 S_{13}^2 C_{12} + S_{12}^2 S_{13}^2 \cancel{C_{12}} + \cancel{S_{12}^2 S_{13}^2 C_{23}}] [C_{13}^2 S_{23} C_{23}] \\
 &= -4[-S_{23} C_{23} + C_{12}^2 S_{13}^2 C_{23} + S_{12}^2 S_{23} S_{23}] [C_{13}^2 S_{23} C_{23}] \\
 &= -4[-1 + C_{12}^2 S_{13}^2 + S_{12}^2 S_{13}^2] [C_{13}^2 S_{23}^2 C_{23}^2] \\
 &= -4[-1 + S_{13}^2 (C_{12}^2 + S_{12}^2)] [\dots] \\
 &= -4[S_{13}^2 - 1] [C_{13}^2 S_{23}^2 C_{23}^2] \\
 &= 4 C_{13}^4 S_{23}^2 C_{23}^2 \\
 &= C_{13}^4 \sin^2(2\theta_{23})
 \end{aligned}$$

$$\begin{aligned}
 P(\mu \rightarrow \mu) &= 1 - [\sin^2(\theta_{23}) \sin^2(2\theta_{13}) + \cos^4(\theta_{13}) \sin^2(2\theta_{23})] \sin^2(1.27 \Delta m_{23}^2 \frac{L}{E}) \\
 &= 1 - [A \sin^2(2\theta_{23}) + B(1 - \sin^2\theta_{13})^2] \\
 &\quad + B(1 + \sin^4(\theta_{13}) - 2\sin^2\theta_{13})
 \end{aligned}$$

Additional 2 flavour oscillation derivation (rough notes)

$$|\nu_\alpha(x, t)\rangle = U_{\alpha i} |\nu_i(x, t)\rangle$$

$$\begin{pmatrix} \nu_e \\ \nu_\mu \\ \nu_\tau \end{pmatrix} = \begin{pmatrix} U_{e1} & U_{e2} & U_{e3} \\ U_{\mu 1} & U_{\mu 2} & U_{\mu 3} \\ U_{\tau 1} & U_{\tau 2} & U_{\tau 3} \end{pmatrix} \begin{pmatrix} \nu_1 \\ \nu_2 \\ \nu_3 \end{pmatrix} \rightarrow \begin{pmatrix} \nu_e(x, t) \\ \nu_\mu(x, t) \\ \nu_\tau(x, t) \end{pmatrix} = \begin{pmatrix} e^{-i\phi_1} & 0 & 0 \\ 0 & e^{-i\phi_2} & 0 \\ 0 & 0 & e^{-i\phi_3} \end{pmatrix} \begin{pmatrix} \nu_1(0, 0) \\ \nu_2(0, 0) \\ \nu_3(0, 0) \end{pmatrix}$$

$$\begin{pmatrix} \nu_e \\ \nu_\mu \\ \nu_\tau \end{pmatrix} = U_{(3)} \begin{pmatrix} \nu_1 \\ \nu_2 \\ \nu_3 \end{pmatrix}$$

$$\begin{pmatrix} \nu_1 \\ \nu_2 \\ \nu_3 \end{pmatrix} = U_3^{-1} \begin{pmatrix} \nu_e(0, 0) \\ \nu_\mu(0, 0) \\ \nu_\tau(0, 0) \end{pmatrix}$$

$$\boxed{\begin{pmatrix} \nu_e(x, t) \\ \nu_\mu(x, t) \\ \nu_\tau(x, t) \end{pmatrix} = U_{(3)} \begin{pmatrix} e^{-i\phi_1} & 0 & 0 \\ 0 & e^{-i\phi_2} & 0 \\ 0 & 0 & e^{-i\phi_3} \end{pmatrix} \begin{pmatrix} \nu_e(0, 0) \\ \nu_\mu(0, 0) \\ \nu_\tau(0, 0) \end{pmatrix}}$$

$$P(e \rightarrow \mu) = \langle \nu_\mu(x, t) | \nu_e(0, 0) \rangle$$

$$P(e \rightarrow \mu) \stackrel{\text{Aim}}{=} |U_{e1} U_{\mu 1}^* e^{-i\phi_1} + U_{e2} U_{\mu 2}^* e^{-i\phi_2} + U_{e3} U_{\mu 3}^* e^{-i\phi_3}|^2$$

$$\det(U_{(3)}) = U_{e1}(U_{\mu 2} U_{\tau 3} - U_{\mu 3} U_{\tau 2})$$

$$\begin{pmatrix} |\nu_e(0, 0)\rangle \\ |\nu_\mu(0, 0)\rangle \end{pmatrix} = \begin{pmatrix} \cos\theta & \sin\theta \\ \sin\theta & \cos\theta \end{pmatrix} \begin{pmatrix} |\nu_1(0, 0)\rangle \\ |\nu_2(0, 0)\rangle \end{pmatrix}$$

$$\begin{pmatrix} |\nu_1(0, 0)\rangle \\ |\nu_2(0, 0)\rangle \end{pmatrix} = \begin{pmatrix} \cos\theta & -\sin\theta \\ \sin\theta & \cos\theta \end{pmatrix} \begin{pmatrix} |\nu_e(0, 0)\rangle \\ |\nu_\mu(0, 0)\rangle \end{pmatrix}$$

$$\begin{pmatrix} |\nu_1(x, t)\rangle \\ |\nu_2(x, t)\rangle \end{pmatrix} = \begin{pmatrix} e^{-i\phi_1} & 0 \\ 0 & e^{-i\phi_2} \end{pmatrix} \begin{pmatrix} \cos\theta & -\sin\theta \\ \sin\theta & \cos\theta \end{pmatrix} \begin{pmatrix} |\nu_e(0, 0)\rangle \\ |\nu_\mu(0, 0)\rangle \end{pmatrix}$$

$$\begin{pmatrix} |\nu_1(x, t)\rangle \\ |\nu_2(x, t)\rangle \end{pmatrix} = \begin{pmatrix} e^{-i\phi_1} & 0 \\ 0 & e^{-i\phi_2} \end{pmatrix} \begin{pmatrix} \cos\theta & -\sin\theta \\ \sin\theta & \cos\theta \end{pmatrix} \begin{pmatrix} |\nu_e(0, 0)\rangle \\ |\nu_\mu(0, 0)\rangle \end{pmatrix}$$

$$\begin{pmatrix} v_e(x, t) \\ v_m(x, t) \end{pmatrix} = \begin{pmatrix} \cos \theta & \sin \theta \\ -\sin \theta & \cos \theta \end{pmatrix} \underbrace{\begin{pmatrix} e^{-i\phi_1} & 0 \\ 0 & e^{-i\phi_2} \end{pmatrix}}_{\begin{pmatrix} \cos \phi_1 & -\sin \phi_1 \\ \sin \phi_1 & \cos \phi_1 \end{pmatrix}} \begin{pmatrix} \cos \theta & -\sin \theta \\ \sin \theta & \cos \theta \end{pmatrix} \begin{pmatrix} v_e(0, 0) \\ v_m(0, 0) \end{pmatrix}$$

$$\begin{pmatrix} v_e(x, t) \\ v_m(x, t) \end{pmatrix} = \begin{pmatrix} e^{-i\phi_1} \cos \theta & -e^{-i\phi_1} \sin \theta \\ e^{-i\phi_2} \sin \theta & e^{-i\phi_2} \cos \theta \end{pmatrix} \begin{pmatrix} v_e(0, 0) \\ v_m(0, 0) \end{pmatrix}$$

$$\begin{pmatrix} v_e(x, t) \\ v_m(x, t) \end{pmatrix} = \begin{pmatrix} e^{-i\phi_1} c^2 + e^{-i\phi_2} s^2 & -c \sin \phi_1 + c \sin \phi_2 \\ -c \sin \phi_1 + c \sin \phi_2 & s^2 e^{-i\phi_1} + c^2 e^{-i\phi_2} \end{pmatrix} \begin{pmatrix} v_e(0, 0) \\ v_m(0, 0) \end{pmatrix}$$

$$P(e \rightarrow \mu) = |\langle v_m(x, t) | v_e(0, 0) \rangle|^2$$

$$\begin{aligned}
 & \left| \langle (-c s e^{-i\phi_1} + c s e^{-i\phi_2}) v_e(0, 0) + (s^2 e^{-i\phi_1} + c^2 e^{-i\phi_2}) v_m(0, 0) \mid v_e(0, 0) \rangle \right|^2 \\
 &= \left| (-c s e^{-i\phi_1} + c s e^{-i\phi_2}) \right|^2 |v_e(0, 0)|^2 \\
 &= C^2 s^2 + C^2 s^2 - C^2 s^2 e^{-i\phi_1} e^{i\phi_2} - C^2 s^2 e^{i\phi_1} e^{-i\phi_2} \\
 &= C^2 s^2 (2 - e^{-i\phi_1} e^{i\phi_2} - e^{i\phi_1} e^{-i\phi_2}) \\
 &= 1 - e^{i\phi_2} e^{-i\phi_1} - e^{i\phi_1} e^{-i\phi_2} + 1 \\
 P(e \rightarrow \mu) &= C^2 s^2 \underbrace{|e^{i\phi_2} - e^{i\phi_1}|^2}_{=1} (e^{-i\phi_2} - e^{-i\phi_1}) (e^{i\phi_2} - e^{i\phi_1})
 \end{aligned}$$

$$\cos \theta \sin \theta = \frac{1}{2} \sin 2\theta$$

$$\cos^2 \theta \sin^2 \theta = \frac{1}{4} \sin^2 2\theta$$

$$\sin x = \frac{e^x - e^{-x}}{2i}$$

$$\sin^2 x = \frac{|e^x - e^{-x}|^2}{4}$$

$$x = \frac{\phi_2 - \phi_1}{2}$$

$$P(e \rightarrow \mu) = \sin^2(2\theta) \sin^2\left(\frac{\phi_2 - \phi_1}{2}\right)$$

$$\begin{aligned}
 & \left| e^{\frac{i\phi_2}{2}} e^{\frac{i\phi_1}{2}} \left(e^{\frac{i\phi_2}{2}} e^{\frac{-i\phi_1}{2}} - e^{\frac{-i\phi_2}{2}} e^{\frac{i\phi_1}{2}} \right) \right|^2 \\
 &= \left| e^{\frac{i(\phi_1 + \phi_2)}{2}} \right|^2 \left| e^{\frac{i(\phi_2 - \phi_1)}{2}} - e^{\frac{-i(\phi_2 - \phi_1)}{2}} \right|^2 \\
 &= 4 \sin^2\left(\frac{\phi_2 - \phi_1}{2}\right)
 \end{aligned}$$

but why $e^{-i\phi_2 - \phi_1}$?

$$P^2 = E_i^2 - m_i^2$$

$$P \cdot E_i \left(1 - \frac{m_i^2}{E_i^2}\right)$$

$$\approx E_i \left(1 - \frac{m_i^2}{2E_i^2}\right)$$

$$P \approx E_i - \frac{m_i^2}{2E_i}$$

$$g_i \cdot x = E_i t - P \cdot x$$

$$g_i \cdot x = E_i t - E_i x + \frac{m_i^2}{2E_i} x$$

$$\text{Assume } t \gg x$$

$$g_i \cdot x = \frac{m_i^2}{2E_i} x$$

$$\sin^2(2\theta) \sin^2\left(\frac{1}{4E} (m_2^2 - m_1^2) L\right)$$

$$P(e \rightarrow \mu) = \sin^2(2\theta) \sin^2\left(\frac{\Delta m_{21}^2}{4E} L\right)$$

$$P(e \rightarrow e) = 1 - P(e \rightarrow \mu)$$

All Code for this Lab is located in: '/usr/harrytabb/documents/Lab2/mainanalysis.ipynb'

All figures for this Lab are located in: '/usr/harrytabb/documents/Lab2'